Aromatic Hydroxylation Reactivity of a Mononuclear Cu(II)−Alkylperoxo Complex

ARTICLE *in* JOURNAL OF THE AMERICAN CHEMICAL SOCIETY · JULY 2007

Impact Factor: 12.11 · DOI: 10.1021/ja071623g · Source: PubMed

7 AUTHORS, INCLUDING:

Christopher J Cramer
University of Minnesota Twin Cities
531 PUBLICATIONS **23,167** CITATIONS
SEE PROFILE

Shinobu Itoh
Osaka University
230 PUBLICATIONS **4,972** CITATIONS
SEE PROFILE

J|A|C|S
COMMUNICATIONS

Published on Web 05/16/2007

Aromatic Hydroxylation Reactivity of a Mononuclear Cu(II)−Alkylperoxo Complex

Atsushi Kunishita,[†] Junji Teraoka,[†] Joseph D. Scanlon,[‡] Takahiro Matsumoto,[§] Masatatsu Suzuki,[§] Christopher J. Cramer,[‡] and Shinobu Itoh*,[†]

Departments of Chemistry and Material Sciences, Graduate School of Science, Osaka City University, 3-3-138 Sugimoto, Sumiyoshi-ku, Osaka 558-8585, Japan, Department of Chemistry and Supercomputer Institute, University of Minnesota, 207 Pleasant Street SE, Minneapolis, Minnesota 55455, and Division of Material Sciences, Graduate School of Natural Science and Technology, Kanazawa University, Kakuma-machi, Kanazawa 920-1192, Japan

Received March 16, 2007; E-mail: shinobu@sci.osaka-cu.ac.jp

The reactions of copper(II) complexes and hydrogen peroxide (H_2O_2) have been studied extensively in order to gain insight into reactive intermediates involved in copper monooxygenases and copper oxidases as well as copper-catalyzed oxidation reactions.[1−19] Several types of mononuclear and dinuclear copper/active-oxygen complexes have been reported, and their structures and physicochemical properties have been explored in detail.[1−19] However, less is known about the intrinsic reactivity of the generated copper/active-oxygen complexes.

We herein report a new copper(II)−alkylperoxo species $\mathbf{2^X}$ [2-hydroxy-2-hydroperoxypropane (HHPP) adduct], which is generated by the reaction of H_2O_2 and copper(II) complex $\mathbf{1^X}$ supported by the bis(pyridylmethyl)amine tridentate ligand containing *m*-substituted phenyl groups at the 6-positions of the pyridine rings (L^X) in acetone in the presence of triethylamine (NEt_3) (Scheme 1). The alkylperoxo intermediate $\mathbf{2^X}$ undergoes an efficient aromatic ligand hydroxylation reaction, producing phenolate complex $\mathbf{4^X}$ via another intermediate $\mathbf{3^X}$. Kinetic studies on the aromatic hydroxylation process are reported here together with spectral characterization of $\mathbf{2^X}$.

Starting mononuclear copper(II) complexes $\mathbf{1^X}$ supported by ligand L^X (X = NO_2, Cl, H, Me, or OMe; Y = ClO_4^- or H_2O; S = CH_3CN or H_2O) were prepared by mixing the ligands and Cu$(ClO_4)_2$·$6H_2O$ in acetone or acetonitrile (Figures S1−S4).[20] The reaction of $\mathbf{1^X}$ and H_2O_2 (1 equiv) was then examined in acetone at −70 °C in the presence of triethylamine (1 equiv). Figure 1A shows a spectral change for the reaction of $\mathbf{1^{NO_2}}$ as a typical example, where intermediate $\mathbf{2^{NO_2}}$ exhibiting a characteristic absorption band at 420 nm (ϵ = 1350 M^{-1} cm^{-1}) together with a weak d−d band at 630 nm (ϵ = 200 M^{-1} cm^{-1}) becomes apparent. Spectroscopic titration for the generation of $\mathbf{2^{NO_2}}$ established that the stoichiometry of $\mathbf{1^{NO_2}}$ to H_2O_2 was 1:1 (Figure S5). Similar spectral changes were obtained with other ligand systems (Figures S6−S9). A more detailed characterization of intermediate $\mathbf{2^X}$ was carried out for $\mathbf{2^{NO_2}}$ since it showed higher stability than any other (as discussed further below).

Intermediate $\mathbf{2^{NO_2}}$ generated with $H_2{}^{16}O_2$ showed isotope sensitive Raman bands at 855, 823, 792, and 545 cm^{-1} when an acetone-d_6 (CD_3COCD_3) solution of $\mathbf{2^{NO_2}}$ was excited with a 441.6 nm laser light (Figure S10). These Raman bands shifted to 825, 803, 785, and 525 cm^{-1}, respectively, when $H_2{}^{18}O_2$ was used (Figure S10). The appearance of multiple Raman bands in the 800 cm^{-1} region and their associated isotope shifts ($\Delta\nu$ = 30, 20, and 7 cm^{-1}) as well as their intensity patterns are similar to those reported from

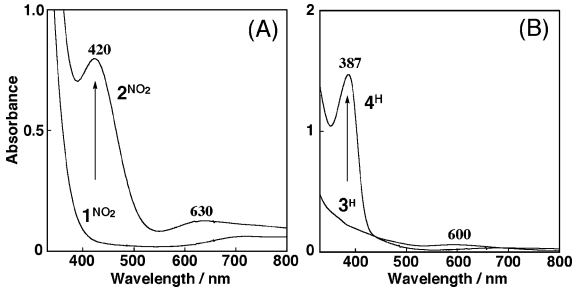

Figure 1. (A) UV−vis spectra of $\mathbf{1^{NO_2}}$ (0.6 mM) and $\mathbf{2^{NO_2}}$ from the reaction of $\mathbf{1^{NO_2}}$ and H_2O_2 (0.6 mM) in the presence of NEt_3 (0.6 mM) in acetone at −70 °C. (B) UV−vis spectra of $\mathbf{3^H}$ and $\mathbf{4^H}$ generated by decomposition of $\mathbf{2^H}$ in acetone.

Scheme 1

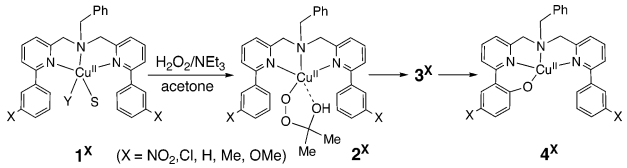

resonance Raman studies of copper(II)−alkylperoxo (Cu^{II}−OOR) and iron(III)−alkylperoxo (Fe^{III}−OOR) complexes (R = *tert*-butyl and cumyl), where such bands have been assigned as mixed O−O/C−O/C−C vibrations.[9,21,22] An additional Raman band of $\mathbf{2^{NO_2}}$ at 545 cm^{-1} ($^{18}\Delta\nu$ = 20 cm^{-1}) can be assigned to a Cu−O stretching vibration (Figure S10). These Raman features are consistent with the formation of a copper(II)−alkylperoxo type species. If $\mathbf{2^{NO_2}}$ were instead to be a copper(II)−hydroperoxo species, Cu(II)−OOH, the Raman spectrum should be much simpler, showing only one peak near 800 cm^{-1} due to the O−O bond stretching vibration.[1−19]

A plausible structure of copper(II)−alkylperoxo complex $\mathbf{2^{NO_2}}$ is a 2-hydroxy-2-hydroperoxypropane (HHPP) adduct as indicated in Scheme 1. A similar HHPP adduct of iron(III) has recently been reported by Que and co-workers in the reaction of Fe^{II}(TPA) and H_2O_2 in acetone.[23,24] The proposed structure of $\mathbf{2^{NO_2}}$ is consistent with the sensitivity of the resonance Raman bands at 855 and 823 cm^{-1} using acetone-d_6 versus acetone-h_6 (CH_3COCH_3; other peaks observed in acetone-d_6 were masked by the large solvent vibration peaks in acetone-h_6; Figure S11), which provides evidence for the incorporation of an acetone molecule into $\mathbf{2^{NO_2}}$. In addition, the ESI-MS of $\mathbf{2^{NO_2}}$ showed a set of peaks at 685.1 which shifted to 689.1 upon $H_2{}^{18}O_2$ substitution (Figure S12). The mass distribution patterns and the isotope shift are fully consistent with the proposed structure of $\mathbf{2^{NO_2}}$. The ESR spectrum of $\mathbf{2^{NO_2}}$ (Figure S14, g_1 = 2.315, g_2 = 2.110, g_3 = 2.035, A_1 = 135, A_2 = 25, A_3 = 30 G), which is different from that of starting material $\mathbf{1^{NO_2}}$ (Figure S13,

[†] Osaka City University.
[‡] University of Minnesota.
[§] Kanazawa University.

10.1021/ja071623g CCC: $37.00

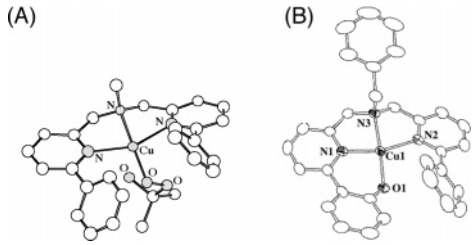

Figure 2. (A) Computed B98 structure for $\mathbf{2^H}$ (*N*-benzyl group is replaced with a methyl group for simplicity) and (B) ORTEP drawing of $\mathbf{4^H}$ showing 50% probability thermal ellipsoids. The counteranion and the hydrogen atoms are omitted for clarity.

$g_1 = 2.310$, $g_2 = 2.100$, $g_3 = 2.030$, $A_1 = 140$, $A_2 = 22$, $A_3 = 24$ G), indicates a distorted tetragonal structure. Moreover, double integration of the ESR spectrum of $\mathbf{2^{NO_2}}$ indicated that 99% of spin remained, confirming the mononuclearity of $\mathbf{2^{NO_2}}$. Finally, B98 density functional calculations predict a stationary structure for $\mathbf{2^{NO_2}}$ (Figure 2A) whose spectral characteristics are in good accord with experiment.[25]

The HHPP adduct $\mathbf{2^X}$ gradually decomposed at −70 °C, resulting in the formation of another intermediate $\mathbf{3^X}$ having a featureless UV/vis spectrum (Figure 1B; the spectrum of $\mathbf{3^H}$ is presented as a typical example). The reaction of $\mathbf{2^H}$ to $\mathbf{3^H}$ obeyed first-order kinetics (Figure S15), and from the temperature dependence of the decay rate, we obtained the activation parameters $\Delta H^{\ddagger} = 24.9 \pm 1.2$ kJ mol^{-1} and $\Delta S^{\ddagger} = -162.9 \pm 5.5$ J K^{-1} mol^{-1} (Figure S16). Furthermore, Hammett analysis (plot of log k_{obs} vs σ^+) gave $\rho = -2.2$ ($r^2 = 0.99$) (Figure S17), which is very close to the ρ values reported for aromatic hydroxylation reactions of dicopper(II)−peroxo complexes (−1.8 to −2.2).[26−28] In addition, no kinetic deuterium isotope effect (KIE = 1.0) was obtained with perdeuterated ligand L^H-d_{10} (replacing all protons of the 6-phenyl groups). These kinetic results suggest that the reaction of $\mathbf{2^X}$ to $\mathbf{3^X}$ involves an electrophilic aromatic substitution mechanism.

Intermediate $\mathbf{3^X}$ further reacted at higher temperature to give the final product $\mathbf{4^X}$ exhibiting an intense absorption band at ∼380 nm (the spectrum of $\mathbf{4^H}$ is shown in Figure 1B, and those of other $\mathbf{4^X}$ are presented in Figures S19−S22). The ESI-MS of the final reaction mixture with $H_2{}^{16}O_2$ and $H_2{}^{18}O_2$ (Figure S23) showed, respectively, increments of 15 and 17 mass units relative to $\mathbf{1^H}$, demonstrating incorporation of one oxygen atom into the product. Aromatic ligand hydroxylation was unambiguously confirmed by single-crystal X-ray structural analysis of the isolated copper(II)−phenolate complex $\mathbf{4^H}$ (Figure 2B) and by ^{1}H NMR analysis on the modified ligands L^X−OH isolated by demetalation of the final products $\mathbf{4^X}$. The yields of ligand hydroxylation were 99, 98, 85, 99, and 53% for X = OMe, Me, H, Cl, and NO_2, respectively.

In summary, we have demonstrated a unique reactivity of copper(II) complexes $\mathbf{1^X}$ with H_2O_2 in acetone via the intermediacy of a new copper(II)−alkylperoxo complex $\mathbf{2^X}$. The alkylperoxo complex $\mathbf{2^X}$ is electrophilic in nature ($\rho = -2.2$) and accomplishes aromatic ligand hydroxylation. In other solvent systems such as propionitrile, by contrast, we observed formation of copper(II)−hydroperoxo species, Cu^{II}−OOH (360 nm, $\epsilon = 3150$ M^{-1} cm^{-1}), from which no aromatic ligand hydroxylation took place. Thus, the present study offers important insights into solvent effects on the reactivity of copper(II) complexes when mixed with H_2O_2. The structure of intermediate $\mathbf{3^X}$ and the mechanism for its formation is now under investigation by experiment and computation.[29]

Acknowledgment. Dedicated to the memory of Professor Yoshihiko Ito. This work was financially supported in part by Grants-in-Aid for Scientific Research (Nos. 17350086, 18037062, and 18033045 for S.I.; Nos. 16350030 and 16074206 for M.S.) from MEXT and JSPS, Japan and the U.S. National Science Foundation (CHE-0610183 for C.J.C.).

Supporting Information Available: Experimental details for the synthetic procedures, computational methods, crystal structures of $\mathbf{1^X}$ and $\mathbf{4^H}$ (ORTEP drawings and CIF data), and additional spectroscopic and kinetic data. This material is available free of charge via the Internet at http://pubs.acs.org.

References

(1) Itoh, S. *Curr. Opin. Chem. Biol.* **2006**, *10*, 115−122.
(2) Ohtsu, H.; Itoh, S.; Nagatomo, S.; Kitagawa, T.; Ogo, S.; Watanabe, Y.; Fukuzumi, S. *Inorg. Chem.* **2001**, *40*, 3200−3207.
(3) Osako, T.; Nagatomo, S.; Tachi, Y.; Kitagawa, T.; Itoh, S. *Angew. Chem., Int. Ed.* **2002**, *41*, 4325−4328.
(4) Osako, T.; Nagatomo, S.; Kitagawa, T.; Cramer, C. J.; Itoh, S. *J. Biol. Inorg. Chem.* **2005**, *10*, 581−590.
(5) Shimokawa, C.; Teraoka, J.; Tachi, Y.; Itoh, S. *J. Inorg. Biochem.* **2006**, *100*, 1118−1127.
(6) Li, L.; Narducci Sarjeant, A. A.; Karlin, K. D. *Inorg. Chem.* **2006**, *45*, 7160−7172.
(7) Lee, Y.; Lee, D.-H.; Narducci Sarjeant, A. A.; Zakharov, L. N.; Rheingold, A. L.; Karlin, K. D. *Inorg. Chem.* **2006**, *45*, 10098−10107.
(8) Kitajima, N.; Fujisawa, K.; Fujimoto, C.; Moro-oka, Y.; Hashimoto, S.; Kitagawa, T.; Toriumi, K.; Tatsumi, K.; Nakamura, A. *J. Am. Chem. Soc.* **1992**, *114*, 1277−1291.
(9) Chen, P.; Fujisawa, K.; Solomon, E. I. *J. Am. Chem. Soc.* **2000**, *122*, 10177−10193.
(10) Wada, A.; Harata, M.; Hasegawa, K.; Jitsukawa, K.; Masuda, H.; Mukai, M.; Kitagawa, T.; Einaga, H. *Angew. Chem., Int. Ed.* **1998**, *37*, 798−799.
(11) Fujii, T.; Naito, A.; Yamaguchi, S.; Wada, A.; Funahashi, Y.; Jitsukawa, K.; Nagatomo, S.; Kitagawa, T.; Masuda, H. *Chem. Commun.* **2003**, 2700−2701.
(12) Yamaguchi, S.; Nagatomo, S.; Kitagawa, T.; Funahashi, Y.; Ozawa, T.; Jitsukawa, K.; Masuda, H. *Inorg. Chem.* **2003**, *42*, 6968−6970.
(13) Yamaguchi, S.; Masuda, H. *Sci. Technol. Adv. Mater.* **2005**, *6*, 34−47.
(14) Kodera, M.; Tachi, Y.; Hirota, S.; Katayama, K.; Simakoshi, H.; Kano, K.; Fujisawa, K.; Moro-oka, Y.; Naruta, Y.; Kitagawa, T. *Chem. Lett.* **1998**, 389−390.
(15) Kodera, M.; Kita, T.; Miura, I.; Nakayama, N.; Kawata, T.; Kano, K.; Hirota, S. *J. Am. Chem. Soc.* **2001**, *123*, 7715−7716.
(16) Itoh, K.; Hayashi, H.; Furutachi, H.; Matsumoto, T.; Nagatomo, S.; Tosha, T.; Terada, S.; Fujinami, S.; Suzuki, M.; Kitagawa, T. *J. Am. Chem. Soc.* **2005**, *127*, 5212−5223.
(17) Mizuno, M.; Honda, K.; Cho, J.; Furutachi, H.; Tosha, T.; Matsumoto, T.; Fujinami, S.; Kitagawa, T.; Suzuki, M. *Angew. Chem., Int. Ed.* **2006**, *45*, 6911−6914.
(18) Ohta, T.; Tachiyama, T.; Yoshizawa, K.; Yamabe, T.; Uchida, T.; Kitagawa, T. *Inorg. Chem.* **2000**, *39*, 4358−4369.
(19) Battaini, G.; Monzani, E.; Perotti, A.; Para, C.; Casella, L.; Santagostini, L.; Gullotti, M.; Dillinger, R.; Näther, C.; Tuczek, F. *J. Am. Chem. Soc.* **2003**, *125*, 4185−4198.
(20) Experimental details of the synthetic procedures are provided in Supporting Information. Details of the X-ray crystallographic analyses of the copper(II) complexes are also provided in Supporting Information (CIF format).
(21) Zang, Y.; Elgren, T. E.; Dong, Y.; Que, L., Jr. *J. Am. Chem. Soc.* **1993**, *115*, 811−813.
(22) Zang, Y.; Kim, J.; Dong, Y.; Wilkinson, E. C.; Appelman, E. H.; Que, L., Jr. *J. Am. Chem. Soc.* **1997**, *119*, 4197−4205.
(23) Payeras, A. M.; Ho, R. Y. N.; Fujita, M.; Que, L., Jr. *Chem.−Eur. J.* **2004**, *10*, 4944−4953.
(24) The reversible addition of H_2O_2 to acetone to form 2-hydroxy-2-hydroperoxypropane (HHPP) was first studied in detail by Sauer, M. C. V.; Edwards, J. O. *J. Phys. Chem.* **1971**, *75*, 3004−3011.
(25) Computational methods are described in the Supporting Information. Predicted O−O/C−O/C−C/Cu−O vibrational frequencies are 901, 814, 700, and 545 cm^{-1} with corresponding isotope shifts of 35, 23, 6, and 24 cm^{-1} (mean unsigned error compared to experiment of 39 and 3 cm^{-1}, respectively). TDDFT computations predict strong and weak absorption maxima at approximately 450 and 620 nm, respectively.
(26) Itoh, S.; Kumei, H.; Taki, M.; Nagatomo, S.; Kitagawa, T.; Fukuzumi, S. *J. Am. Chem. Soc.* **2001**, *123*, 6708−6709.
(27) Palavicini, S.; Granata, A.; Monzani, E.; Casella, L. *J. Am. Chem. Soc.* **2005**, *127*, 18031−18036.
(28) Matsumoto, T.; Furutachi, H.; Kobino, M.; Tomii, M.; Nagatomo, S.; Tosha, T.; Osako, T.; Fujinami, S.; Itoh, S.; Kitagawa, T.; Suzuki, M. *J. Am. Chem. Soc.* **2006**, *128*, 3874−3875.
(29) ESR data for $\mathbf{3^H}$ are presented in Figure S18. The acquisition of a resonance Raman spectrum has not yet proven possible.

JA071623G